In vivo reconstitution of a homodimeric cytochrome b_{559} like structure: The role of the N-terminus α-subunit from *Synechocystis sp.* PCC 6803.

María A. Luján[1], Jesús I. Martínez[2], Pablo J. Alonso[2], Alejandro Torrado[3], Mercedes Roncel[3], José M. Ortega[3], Javier Sancho[4] and Rafael Picorel[1]

[1]Estación Experimental Aula Dei (EEAD), Consejo Superior de Investigaciones Científicas (CSIC), Carretera Montañana 1005, 50059 Zaragoza, Spain.

[2]Instituto Ciencia de Materiales de Aragón (ICMA) (CSIC-Universidad de Zaragoza), C/Pedro Cerbuna 12, 50009 Zaragoza, Spain.

[3]Instituto de Bioquímica Vegetal y Fotosíntesis (IBVF) (Universidad de Sevilla-CSIC), Avda. Américo Vespucio 49, 41092 Sevilla, Spain.

[4]Instituto de Biocomputación y Física de Sistemas Complejos - Unidad BIFI-IQFR (CSIC) (Universidad de Zaragoza), C/ Mariano Esquilar s/n, 50018 Zaragoza, Spain. Departamento de Bioquímica y Biología Molecular y Celular (Universidad de Zaragoza), Plaza San Francisco s/n, 50009 Zaragoza, Spain.

Corresponding author: Rafael Picorel, Estación Experimental Aula Dei (EEAD), Consejo Superior de Investigaciones Científicas (CSIC), Carretera Montañana 1005, 50059 Zaragoza, Spain. Tel.:+34(976)716053; FAX:+34(976)716145; Email:picorel@eead.csic.es.

Keywords: alpha-helix; cytochrome; membrane; photosynthesis; chimeric protein; protein assembly.

Abbreviations: Abs, absorbance; BCA, bicinchoninic acid; Cyt, cytochrome; D1 and D2, the two core-subunits of the PSII reaction center; *E.*, *Escherichia*; *E*h, ambient redox potential; *E*m, midpoint redox potential; EPR, electron paramagnetic resonance; IPTG, isopropyl β-D-1-thiogalactopyranoside; MBP, maltose-binding protein; MES, 2-(*N*-morpholino)ethanesulfonic acid; PAGE, polyacrylamide gel electrophoresis; PSII, photosystem II; Q_B, secondary quinone acceptor of the reaction center of PSII; SDS, sodium dodecyl sulfate.

Abstract

The cytochrome b_{559} is a heme-bridged heterodimeric protein with two subunits, α and β. Both subunits from *Synechocystis sp.* PCC 6803 have previously been cloned and overexpressed in *Escherichia coli* and *in vivo* reconstitution experiments have been carried out. The formation of homodimers in the bacterial membrane with endogenous heme was only observed in the case of the β-subunit (β/β) but not with the full length α-subunit. In the present work, reconstitution of a homodimer (α/α) cytochrome b_{559} like structure was possible using a chimeric N-terminus α-subunit truncated before the amino acid isoleucine 17, eliminating completely a short amphipathic α-helix that lays on the surface of the membrane. Overexpression and *in vivo* reconstitution in the bacteria was clearly demonstrated by the brownish color of the culture pellet and the use of a commercial monoclonal antibody against the fusion protein carrier, the maltoside binding protein. Moreover, a simple partial purification after membrane solubilization with Triton X-100 confirmed that the overexpressed protein complex corresponded with the maltoside binding protein-chimeric α-subunit cytochrome b_{559} like structure. The features of the new structure were determined by UV-Vis, electron paramagnetic resonance and redox potentiometric techniques. Ribbon representations of all possible structures are also shown to better understand the mechanism of the cytochrome b_{559} maturation in the bacterial cytoplasmic membrane.

1. Introduction

The photosystem II (PSII) is a membrane-bound supercomplex, which function is to extract electrons and protons from water at the lumen side and reduce plastoquinones at the stroma side to generate electron transfer and proton gradient across the thylakoid membranes. Dioxygen is produced as a byproduct of that process and liberated to the atmosphere. The PSII supercomplex is made of many protein subunits, most of them inserted within the thylakoid membranes with α-helix secondary structure conformation (Kamiya et al. 2003; Guskov et al. 2009). The natural cytochrome (Cyt) b_{559} is a heterodimeric (α/β) metalloprotein that co-purify with the D1-D2 heterodimer (called D1-D2-Cyt b_{559} complex) (Nanba and Satoh 1987; Seibert and Picorel 2011). Both cytochrome protein subunits are of chloroplastic origin (α and β subunits are the products of the *psbE* and *psbF* genes, respectively), and span the thylakoid membrane

with a single α-helix. Each subunit contains a histidine that coordinates the heme group towards the stromal side of the thylakoid membrane (Picorel et al. 1994; Koua et al. 2013) making a hexacoordinate low spin iron (Babcock et al. 1985; Stewart and Brudvig 1998; García-Rubio et al. 2003).

Cytochrome b_{559} shows two unique features with respect to other cytochrome *b*-type proteins. Indeed, most of those cytochromes are made of a single polypeptide and their midpoint redox potentials (E_m) vary between -100 and +100 mV (Kaminskaya et al. 1999; Roncel et al. 2003; Shinopoulos and Brudvig 2012). However, the Cyt b_{559} is a heterodimeric (α/β) protein (Nanba and Satoh 1987; Seibert and Picorel 2011) and it can reach an unusually high redox potential up to +400 mV that can widely vary depending on sample preparations and mutations (Kaminskaya et al. 1999; Roncel et al. 2003; Shinopoulos and Brudvig 2012; Ahmad et al. 1993; Guerrero et al. 2013; Guerrero et al. 2014). These two properties make this metalloprotein more elusive and difficult to characterize, and establish its functional role.

The function of the Cyt b_{559} is not well resolved yet but the most accepted hypothesis nowadays considers that it is involved in the photoinhibition/repair cycle of the PSII (Faller et al. 2001; Alfonso et al. 2004; Shinopoulos and Brudvig 2012; Guerrero et al. 2014; Sugiura et al. 2015). Accordingly, this cytochrome would accept electrons from an overreduced acceptor side (acceptor side photoinhibition) or deliver electrons to a deficient electron donor side (donor side photoinhibition) of the PSII. The secondary plastoquinone (Q_B) is most probably the best candidate to donate electrons to the Cyt b_{559} and the β-carotene of the D2 protein to accept electrons from the Cyt b_{559} (Faller et al. 2001; Shinopoulos and Brudvig 2012; Guerrero et al. 2014; Sigiura et al. 2015). Indeed, the heme moiety of this cytochrome is strategically located between the secondary Q_B and the β-carotene in the crystal structure (Guskov et al. 2009; Koua et al. 2013). For such a role, the Cyt b_{559} has to change easily its redox state from reduced high potential to oxidized low potential forms. Such redox variability is actually observed experimentally in many different preparations of PSII and mutants (Roncel et al. 2003; Shinopoulos and Brudvig 2012; Guerrero et al. 2013; Guerrero et al. 2014, Sigiura et al. 2015) though the underline molecular mechanisms for those changes are yet unknown.

In a previous publication (Luján et al. 2012), we described the *in vitro* reconstitution of a Cyt b_{559} like structure using the recombinant subunits from the plant sugar beet overexpressed in *Escherichia (E.) coli* and partially purified from inclusion bodies. Thus homodimeric and heterodimeric Cyt b_{559} like structures were reconstituted using commercial heme with a yield somewhat higher for the heterodimer (*α/β*) form, the natural structure found in the PSII, than for the homodimers (*α/α*; *β/β*) (Luján et al. 2012). *In vivo* reconstitution was also possible within the *E. coli* cytoplasmic membrane overexpressing only the *β*-subunit from the cyanobacterium *Synechocystis sp.* PCC 6803, confirming previous *in vitro* results from chemically synthesized *β*-subunit and free heme (Franke et al. 1999) and *in vivo* results in recombinant *E. coli* cells (Prodöhl et al. 2005). However, *in vivo* reconstitution overexpressing only the cyanobacterial *α*-subunit was unsuccessful, despite that subunit was actually incorporated and stabilized within the bacterial membrane (Luján et al. 2012; Luján 2009). Thus the heme group was not necessary for the incorporation and stabilization of the Cyt b_{559} *α*-subunit within the membrane. No logical explanation for this result was found at that time, considering the high structural homology between *α*- and *β*-subunits. However, a closer examination of the published crystal structure of the PSII core complex from cyanobacteria (Koua et al. 2013; Umena et al. 2011) revealed the presence of a short amphipathic *α*-helix at the out-of-membrane N-terminus of the *α*-subunit just on top of the heme group niche, which is not observed in the N-terminus of the *β*-subunit. The presence of two *α*-helices on the membrane surface on top of the heme group niche of a (*α/α*) homodimer would suggests the existence of a possible steric hindrance for heme incorporation and its coordination with the two histidines during the holoprotein maturation. To confirm this hypothesis, a chimeric N-terminus *psbE* gene was generated and incorporated into *E. coli* competent cells, and the resultant recombinant bacterial cytoplasmic membrane fragments were analyzed by SDS-PAGE, immunoblot, UV-Vis, electron paramagnetic resonance (EPR) and redox titration potentiometry techniques.

2. Materials and Methods

2.1. Cloning and expression in *E. coli* of full length and truncated Cyt b_{559} *α*-subunit from *Synechocystis sp.* PCC 8603

The full length *psbE* gene from the cyanobacterium *Synechocystis sp.* PCC 6803 was cloned and overexpressed as in Luján (2009) and Luján et al. (2012). A chimeric Cyt

b_{559} α-subunit was generated by removing the first sixteen amino acid residues of the N-terminus, thus the new chimeric protein sequence began at the isoleucine 17 (called thereafter SsubαI17 or αI17). To achieve it, the gene was amplified by PCR using genomic DNA with specific primers containing Bam HI site forward primer and Hind III site reverse primer. Then the gene was ligated to the expression vector pMAL-c2X, and the sequence was confirmed by DNA sequencing. The construct will originate a fusion protein containing the maltose binding protein (MBP) and the truncated N-terminus Cyt b_{559} α-subunit. Note that in the *malE* gene of the commercial expression vector pMAL-c2X, a signal sequence leading to periplasmic expression of the final fusion protein has been deleted (for more information see Instruction Manual pMAL System, New England Biolabs). As a consequence, the MBP protein cannot cross the cytoplasmic membrane to the periplasmic space and thus remains in the cytoplasm. The topology of the MBP protein expressed with these vector series has been examined extensively and unambiguously demonstrated that is located in the periplasmic space when the signal sequence is complete (pMAL-p2) but it appears in the cytoplasm when the signal sequence has the above mentioned deletion (pMAL-c2X) (Prodöhl et al. 2005; Kroliczewski et al. 2005; Dreher et al. 2007; Weber and Schneider 2013). According to this information and the structure of our construction, the heme group of the chimeric homodimeric (α/α) Cyt b_{559} like structure has to be located towards the cytoplasmic side of the bacterial membrane. Two more chimeric constructs were obtained at the N-terminus following the same methodology, one without the first eight residues (chimeric SsubαP9 that preserves the short amphipathic α-helix) and the other without the first twelve residues (chimeric SsubαI13 removing about half of the short α-helix).

Protein overexpression in *E. coli* TB1 competent cells was described in detail in Luján (2009) and Luján et al. (2012). Essentially, the overexpression was induced with 0.5 mM isopropyl β-D-1-thiogalactopyranoside (IPTG) at 37 ºC for 3 h or 1 mM IPTG at 18 ºC for 5 h. Cytoplasmic membrane fragments were obtained according to the protocol published in the aforementioned paper. Bacterial cells were broken by sonication and the crude extract was clarified by centrifugation at 10,000 x *g* for 10 min. The supernatant was centrifuged at 100,000 x *g* for 45 min, and the resultant pellet, resuspended in 50 mM HEPES, pH 7.5, corresponded to the cytoplasmic membrane fragments, the material used in the present study.

Total protein content was determined using bicinchoninic acid (BCA) reagent colorimetric method (Pierce Thermo Scientific, Rockford, IL USA). Protein separation was done in SDS-PAGE [12% (w/v) acrylamide, 4 M urea] after denaturation in boiling water bath for 5 min. Then proteins were revealed by Coomassie brilliant blue staining or blotted onto nitrocellulose membrane with a transfer system (Trans-Blot Turbo, BioRad). Membranes were sequentially incubated with commercial mouse monoclonal anti-MBP (New England Biolabs, County Road, Ipswich, MA USA). Secondary antibodies were goat antimouse IgG, coupled to horseradish peroxidase. Blots were finally colorimetrically developed with H_2O_2 and 4-chloro-1-naphthol.

2.2. Cytoplasmic membrane fragment treatment with NaBr or TRIS-HCl

To remove potential peripheral membrane proteins, cytoplasmic membrane samples were incubated with 2 M NaBr or 50 mM TRIS-HCl, pH 8.0, for 30 min at 4 ^{o}C with gentle swirling. The process was stopped by adding equal volume of cold water, and the suspension was ultracentrifuged at 100,000 x g during 45 min to separate the insoluble membrane fraction as pellet from the supernatant, where the removed soluble proteins were recovered. The treatment was repeated once in the same conditions.

2.3. Protein purification

The MBP-chimeric Ssub*α*I17 fusion protein was partially purified from cytoplasmic membranes previously treated with 50 mM TRIS-HCl, pH 8.0, as explained above. Treated membranes were solubilized with 1% (w/v) Triton X-100 in 50 mM HEPES, pH 7.5, at 4 ^{o}C during 30 min with gentle swirling. The resultant suspension was ultracentrifuged at 150,000 x g during 45 min. The supernatant containing the solubilized material was separated from the pellet for further analysis. The pellet was resuspended in buffer 50 mM HEPES, pH 7.5.

2.4. Absorption spectra

UV-Vis absorption spectra in the 500-600 nm were obtained at room temperature with a Beckman DU 640 spectrophotometer (Beckman Coulter, Brea, CA USA) using 1-cm pathlength cuvette. Samples were used as obtained as blank and then reduced with 10 mM sodium dithionite, giving the reduced *minus* oxidized differential absorption spectra directly. Previous blank oxidation with potassium ferricyanide did not result in a higher intensity of the spectral bands, indicating that the cytochrome was fully oxidized

as obtained in the preparation. A differential extinction coefficient ($\varepsilon_{559.5\ nm\ -\ isosbestic\ point}$ = 17.5 mM^{-1} cm^{-1}) (Stewart and Brudvig 1998) of the Cyt b_{559} spectral α-band was used to determine the concentration of the cytochrome in the preparations.

2.5. Electron paramagnetic resonance (EPR)

EPR spectra were recorded with a Bruker ELEXYS E580 spectrometer (Bruker, Karlsruhe, Germany) working at the X-band (frequency around 9.7 GHz). Typical spectra were taken at low temperature (12K) by using an Oxford CF935 liquid helium continuous-flow cryostat (Oxford Instruments, Eynsham, UK). For measurements, microwave power was kept low enough in order to avoid saturation. Typical measuring conditions were: microwave power, 2 x 10^{-2} mW; modulation amplitude, 0.2 mT.

2.6. Redox potential measurements

Potentiometric titrations were carried out basically as described in Luján et al. (2012) and Guerrero et al. (2014). For titrations, samples were suspended in 2.5 mL buffer containing 50 mM MES-NaOH, pH 6.5, and the following redox mediators: 10 µM diaminodurol (E'_{m7} = +260 mV), 10 µM 2,5-dimethyl-*p*-benzoquinone (E'_{m7} = +180 mV), 10 µM *o*-naphtoquinone (E'_{m7} = +145 mV), 2.5 µM N-methyl-phenazonium methosulfate (E'_{m7} = +80 mV) and 10 µM duroquinone (E'_{m7} = +5 mV). Experiments were done at 20 ºC under argon atmosphere and continuous stirring. Reductive titrations were performed by first oxidizing with 25 µM potassium ferricyanide and then reducing it stepwise with small aliquots of 50 mM sodium dithionite. After addition of sodium dithionite, the absorption spectrum between 500-600 nm and the redox potential of the solution were simultaneously recorded by using, respectively, a Hewlett-Packard 8452A diode array UV-Vis spectrophotometer and a Metrohm potentiometer (Metrohm Ltd., Herisau**,** Switzerland) provided with a combined Pt-Ag/AgCl microelectrode (Microelectrodes Inc, Bedford, NH USA), previously calibrated against a saturated solution of quinhydrone (E'_{m7} = +280 mV at 20 ºC). Differential absorption spectra of Cyt b_{559} recorded at each solution redox potential (E_h) were obtained by subtracting the absolute spectra recorded at each E_h during titrations from the spectra of the fully oxidized cytochrome. The absorbance difference at 559 nm *minus* 570 nm obtained from these spectra was converted into percentages of reduced cytochrome and plotted *versus* E_h. The midpoint redox potential (E_m) values were then determined by fitting the Nernst equation for one-electron carrier (n = 1) with 1 or 2 components as needed to the

plots, and using a non-linear curve-fitting option of the Origin 6.0 software (Microcal Software, Piscataway, NJ USA).

2.7. Protein modeling

Sequence alignment of the α- and β-subunits of Cyt b_{559} (corresponding to E and F chains of the X-ray structure of *Thermosynechococcus (T.) vulcanus* PSII core: pdb id = 3ARC) shows that the transmembrane α-helix from each subunit that sandwiches the heme group contains 5 conserved residues (α-subunit R18, H23, P28, F31 and G34, and β-subunit R19, H24, P29, F32 and G35). Inspection of the X-ray structure indicates that those conserved residues contribute as follows to the symmetric arrangement of the helices around the heme. The histidine and arginine residues play key roles in heme binding by coordinating the heme Fe and forming salt bridges with the heme propionic acid side chains, respectively. The small size of the glycine residues allows a close approximation of the two helices at their C-termini, which is reinforced by interhelical contacts between the glycines and phenylalanines. Finally, the prolines force a kink in the helices that allows their better approximation to the intercalated heme. The modeling of the (α/α) dimer was focused in those conserved residues. First, the X-ray structure of the α-subunit was superimposed onto the structure of the β-subunit with *Swiss-pdb viewer* (Guex and Peitsch 1997), using the *fit from selection* choice so that the five conserved residues of the two subunits were optimally superimposed (overall RMSD = 0.87 Å, or 0.25 Å if the more flexible R residue is excluded). Then a new PDB file was built by combining the coordinates of the original α-subunit in 3ARC with those of the α-subunit previously superimposed onto the β-subunit. In this new file the conserved histidine and arginine residues are correctly positioned to interact with the heme group, and the backbone of the modeled α-subunit transmembrane helix closely follows that of the entire original β-subunit helix in the natural Cyt b_{559}. The model was energy minimized with the Gromos96 (van Gunsteren et al. 1996) implementation in *Swiss-pdb viewer* until the computed energy of all side chains reached low values indicative of a lack of clashes. Finally, both the Cyt b_{559} heterodimer (pdb id = 3ARC) and the energy-minimized model of the (α/α) dimer were analyzed with PROCHECK (Laskowski et al. 1993). The various quality scores obtained for the two structures were similar. The model of the truncated (α/α) dimer is based on that of the full length dimer.

The model of the (*β/β*) dimer was done in an analogous manner to that of the (*α/α*) dimer.

3. Results

A ribbon representation of the native Cyt b_{559} structure obtained from the crystal coordinates of the PSII core complex from the cyanobacterium *T. vulcanus* at a resolution of 1.9 Å (Umena et al. 2011) is depicted in the Fig.1. This also shows the N-terminus sequence (shade grey) truncated to obtain the chimeric *α*-subunit from *Synechocystis sp.* PCC 6803 used to transform *E. coli* TB1 competent cells. Pellets from bacterial cultures

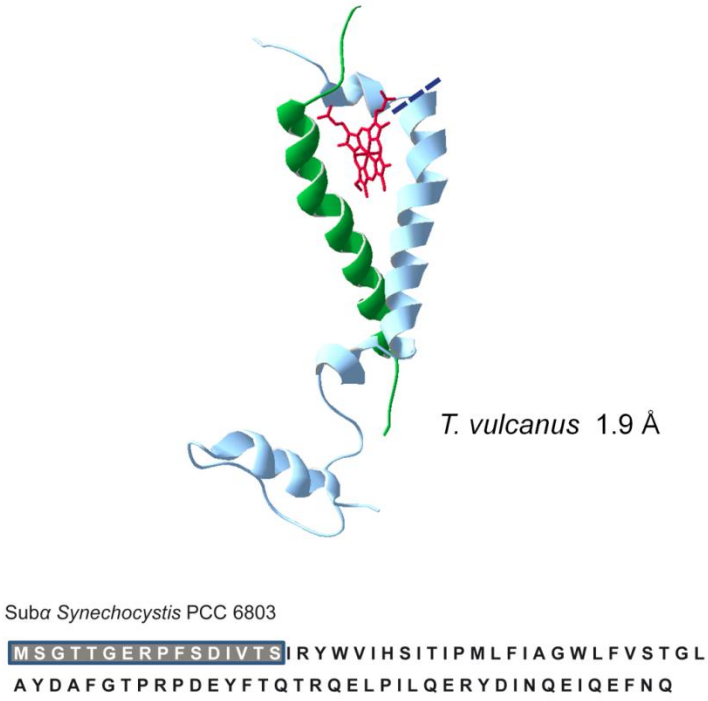

Fig.1*: Structure of the natural heterodimeric (α/β) Cyt b_{559} from cyanobacteria. Upper part, ribbon diagram according to the X-ray crystal structure from T. vulcanus at 1.9 Å resolution: pdb id = 3ARC. Lower part, deduced amino acid sequence of the α-subunit from Synechocystis sp. PCC 6803 where the removed N-terminus part to obtain the chimeric polypeptide appears in shade grey*

transformed with the MBP alone (Fig. 2a, MBP) grown at 37 ^{o}C were colorless as expected. In the overexpression of the full length *α*-subunit at 37 ^{o}C, *E. coli* optimal growth temperature, the bacterial pellet was also colorless and no MBP-Ssub*α* fusion

protein was observed using SDS-PAGE analysis (Luján 2009). We do not have a clear explanation for this result but it could be due to a lesser fusion protein expression, lower protein stability, more prone to protease digestion character, and so forth. To overcome the problem, several growth conditions were tested in this work, and induction at 18 ^{o}C for 5 h were the best conditions found to produce a stable fusion protein. With these new growth conditions, the MBP-full length Ssub*α* fusion protein clearly appeared in the SDS-PAGE at the expected molecular weight, but the pellet from those bacterial cultures still remained colorless (Fig. 2a, *α*), indicating that no reconstitution of a Cyt b_{559} like structure was obtained, despite presence of stable recombinant fusion protein in the membranes. However, cells with the MBP-chimeric *α*-subunit grown both at 18 ^{o}C (Fig. 2a, *α*I17 18 ^{o}C) or 37 ^{o}C (Fig. 2a, *α*I17 37 ^{o}C) showed a distinct brownish color, indicating the reconstitution of a chimeric homodimeric (*α/α*) Cyt b_{559} like structure in *E. coli*. Fig. 2b shows the protein analysis by SDS-PAGE of the membranes obtained from the different cell cultures with empty vector (lane 1), MBP protein alone (lane 2), MBP-full length Ssub*α* fusion protein (lane 3), and MBP-chimeric Ssub*α*I17 fusion protein from cells grown at 18 ^{o}C (lane 4) or 37 ^{o}C (lane 5). Since the chimeric fusion protein appeared somewhat more abundant from cells grown at 37 ^{o}C than at 18 ^{o}C in shorter induction time (3 h *vs* 5 h), we decided to perform the rest of the experiments with membrane fragments obtained from cells grown at 37 ^{o}C induced for 3 h. Note that the apparent molecular weights of the different overexpressed fusion proteins corresponded quite well with the deduced amino acid sequence of the corresponding constructions: MBP + polylinker (19 amino acids) + lacZ alpha peptide: 50,843.27 Da; MBP + polylinker (10 amino acids) + full *α*-subunit from *Synechocystis*: 52,533.28 Da; MBP + polylinker (10 amino acids) + chimeric *α*-subunit I17 from *Synechocystis*: 50,753.30 Da. To better identify them, immunoblot analysis was done using a commercial monoclonal antibody against the MBP protein (Fig. 2c). Thus the results clearly demonstrated that the overexpressed fusion proteins corresponded with the described Coomassie bands, as indicated with arrows in the Fig. 2b and 2c. The presence of some additional immunoreactive bands with close apparent molecular weights could most probably result from slightly different migration in the gel and/or different translation completeness of the overexpressed proteins in the bacteria. We have observed a similar phenomenon using the same protein carrier (MBP) fused to the chloroplastic copper chaperone for the Cu/Zn superoxide dismutase, the CCS (Sagasti et al. 2011). Note that no lower break-down products were detected in the western blot. As

explained in Materials and Methods, the constructions used in this study necessarily resulted in the presence of the MBP protein in the bacterial cytoplasmic space, as

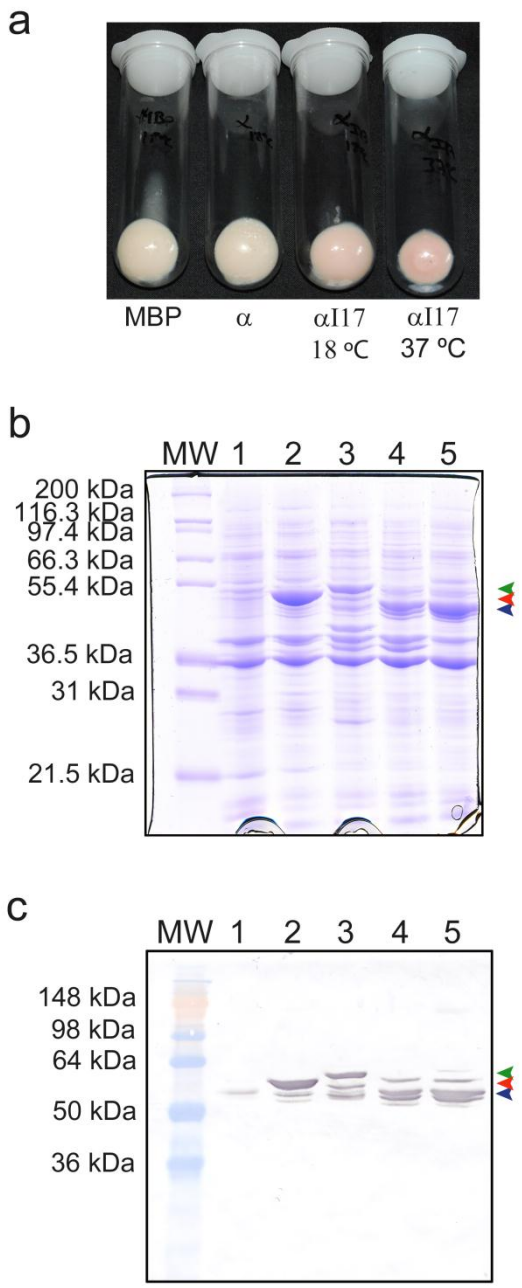

Fig.2*: Overexpresion of fusion proteins. a, pellets of E. coli TB1 cultures: induced at 37 ºC for 3 h containing only the MBP (MBP); induced at 18 ºC for 5 h containing the MBP-full length Ssubα (α); induced at 18 ºC for 5 h containing the MBP-chimeric SsubαI17 (αI17 18 ºC); induced at 37 ºC for 3 h containing the MBP-chimeric SsubαI17*

(αI17 37 ^{o}C). b, SDS-PAGE [12% (w/v) acrylamide, 4 M urea] analysis of bacterial membrane fragments obtained from the pellets described in part a; c, Immunoblots with mouse monoclonal antiMBP antibody. MW, molecular weight markers; lane 1, TB1 bacterial membrane fragments without transformation; lane 2, containing the MBP only (MBP-lacZ fusion protein of 50.8 kDa; red color arrow); lane 3, containing the MBP-full length Ssubα (fusion protein of 52.5 kDa; green color arrow); lane 4, containing the MBP-chimeric SsubαI17 (fusion protein of 50.7 kDa; blue color arrow) at 18 ºC; lane 5, containing the MBP-chimeric SsubαI17 at 37 ºC (fusion protein of 50.7 kDa; blue color arrow)

demonstrated unambiguously in previous works (Prodöhl et al. 2005; Kroliczewski et al. 2005; Dreher et al. 2007; Weber and Schneider 2013) using similar constructs. Thus the heme group of our chimeric Cyt b_{559} like structure has to be necessarily located towards the inner surface of the cytoplasmic membrane. Since the MBP protein is highly overexpressed in our bacterial cultures, it appeared in both soluble and membrane fractions (Luján 2009; Luján et al. 2012). Due to the lack of any clear membrane-spanning element, the MBP protein should be located on the surface as peripheral membrane protein. To prove it, cytoplasmic membranes were treated with NaBr or TRIS-HCl to release the non-integral membrane proteins. SDS-PAGE analysis demonstrated that such treatments indeed released a good part of the MBP protein content from the membranes in the soluble fraction (Fig. 3, lane 2). But a significant fraction of the MBP still remained with the membrane (Fig. 3, lane 3), which would correspond to proteins trapped inside the small membrane vesicle and fragments during the sonication process. Such sonication process would generate a mixture of small membrane vesicle with different surface orientation, and the NaBr or TRIS-HCl treatments would only release the peripheral proteins of the exposed surface.

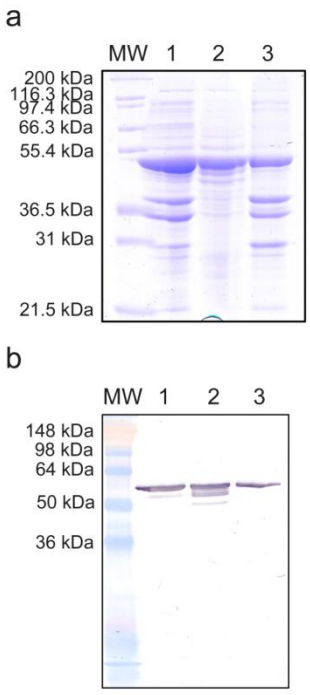

Fig.3*: Membrane fragment treatment with NaBr. Membranes from bacterial cells containing only the MBP protein were treated with 2 M NaBr (similar results were obtained with TRIS-HCl). a, SDS-PAGE Coomassie brilliant blue protein staining; b, Immunoblots using a commercial monoclonal antibody against MBP protein. MW, molecular weight markers; lane 1, control membranes without treatment; lane 2, resultant supernatant after ultracentrifugation; lane 3, resultant pellet after ultracentrifugation*

The degree of overexpression of the Cyt b_{559} like structure can be assessed by the intensity of the visible spectral bands at around 559 nm (α-band) or 530 nm (β-band) after chemical reduction with dithionite. Membranes from control cells (only with MBP) or with full length α-subunit (MBP-Ssubα) showed much smaller spectral band intensities, due to intrinsic bacterial membrane cytochromes, compared to membranes from cells with the chimeric α-subunit (MBP-SsubαI17) both grown at 18 ^{o}C or 37 ^{o}C (Fig. 4), being somewhat higher in the latter and according to the SDS-PAGE analysis (Fig. 2b, lanes 4 and 5).

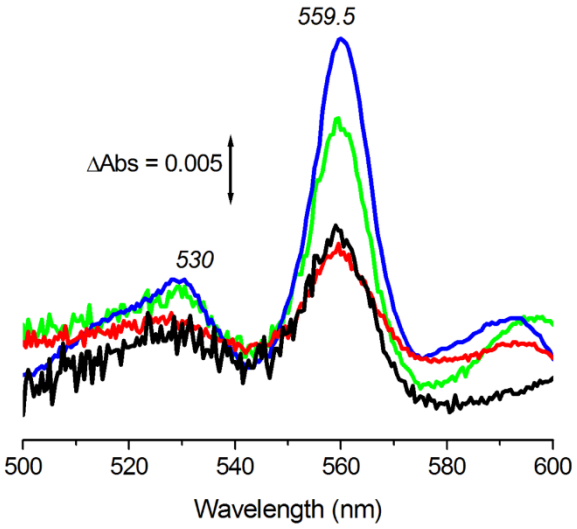

***Fig.4**: Redox differential absorption spectra of the different bacterial cytoplasmic membrane fragments within the 500-600 nm spectral range. a, containing only the MBP (black color line); expressing the MBP-full length Ssubα (red color line); expressing the MBP-chimeric SsubαI17 at 18 ^{o}C (green color line); expressing the MBP-chimeric SsubαI17 at 37 ^{o}C (blue color line). Spectra were normalized to total protein content*

To even better identify the overexpressed chimeric protein as a Cyt b_{559} like structure, a partial purification was attempted using membrane solubilization with Triton X-100. To do that, cytoplasmic membranes, previously treated with 50 mM TRIS-HCl, pH 8.0, were solubilized with 1% (w/v) Triton X-100. The resultant supernatant after ultracentrifugation at 150,000 x g contained most of the overexpressed chimeric protein as shown by SDS-PAGE (Fig. 5a, lane 2; blue color arrow). Surprisingly, most of the other membrane proteins remained in the pellet (Fig. 5b, lane 3), indicating the high efficiency and selectivity of the detergent Triton X-100 extraction. The supernatant depicted a visible absorption spectrum with maximum peaks at around 559 and 530 nm (Fig. 5b), which corresponded well with the spectrum of the native Cyt b_{559}. No spectral signals were observed from the resultant insoluble membrane pellet (Fig. 5b), and according to the SDS-PAGE analysis (Fig. 5a).

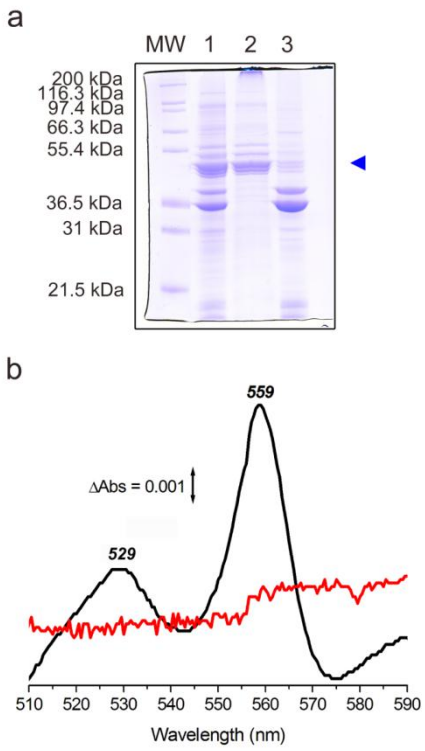

Fig.5*: Partial purification of MBP-chimeric SsubαI17 fusion protein by membrane solubilization with Triton X-100. a, SDS-PAGE [12% (w/v) acrylamide, 4 M urea]: MW, molecular weight markers; lane 1, cytoplasmic membrane fragments previously treated with 50 mM TRIS-HCL, pH 8.0; lane 2, resultant supernatant after ultracentrifugation of detergent solubilized extract; lane 3, resultant pellet after ultracentrifugation. b, redox differential absorption spectra of the supernatant (black color line) and the pellet resuspended in 50 mM HEPES, pH 7.5 (red color line). The arrow indicates the MBP-chimeric SsubαI17 fusion protein*

Since Fe^{3+} ion is a paramagnetic species, EPR is a sound technique to characterize the Cyt b_{559} present in the cytoplasmic membrane fragments. It is well established that the natural heterodimeric Cyt b_{559} is a low spin species with characteristic signals of g_z = 3.0-2.9, g_y = 2.26, and g_x = 1.4 (Babcock et al. 1995; Shuvalov et al. 1995; Stewart and Brudvig 1998; Yruela et al. 2003). Membrane preparation with the MBP protein alone was used as control, and showed almost undetectable EPR spectral signals (Luján et al. 2012). The residual signals would correspond to some endogenous low spin hemoproteins present within the bacterial membrane (Fig. 6, MBP). When membranes with the chimeric fusion protein were used, the spectral features from low spin Cyt b_{559} were now apparent (Fig. 6, *α*I17). When the control was subtracted from this new spectrum (Fig. 4, *α*I17-MBP) and the low spin region expanded (Inset), the presence of low spin Cyt b_{559} was even more apparent. The signals in the spectrum correspond to g

values $g_z = 2.96 \pm 0.03$, $g_y = 2.27 \pm 0.01$, and $g_x = 1.47 \pm 0.05$, fully compatible with a non-distorted Cyt b_{559} species. A signal at around g = 4.3 is due to non-heminic iron centers, and the feature at around g = 6.0 is due to high spin heminic centers. The latter is most probably due to the displacement of one histidine Fe axial ligand by other ligand (Shuvalov et al. 1995), but the concentration of the high spin paramagnetic centers was very low compared to the low spin centers (Luján et al. 2012).

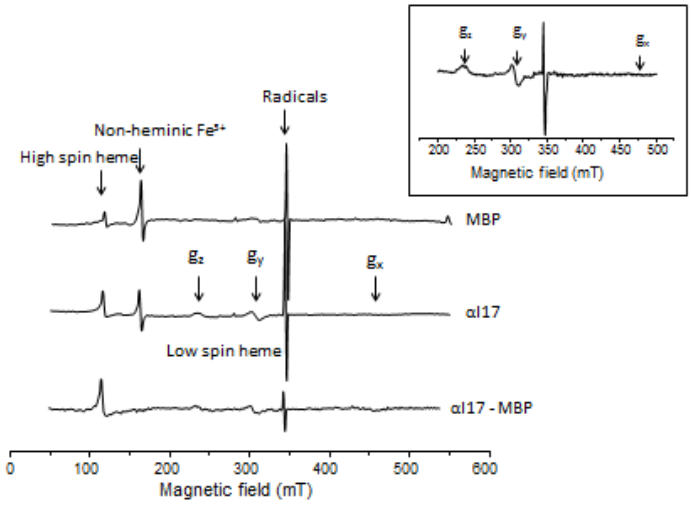

***Fig.6**: X-band EPR spectra of E. coli TB1 cytoplasmic membrane fragments containing MBP protein only, containing the chimeric homodimer (αI17) Cyt b_{559} like structure, and the subtraction of the two spectra (αI17-MBP) (normalized to the g = 4.3 signal height). Spectral features corresponding to high spin heme, non-heminic iron, low spin heme and radicals are indicated. The inset shows a detail of the low spin features from the subtraction spectra that correspond to the Cyt b_{559} low spin features. For experimental conditions, see Materials and Methods section*

The E_m of the *in vivo* reconstituted chimeric homodimeric Cyt b_{559} was measured by potentiometric reductive titrations at pH 6.5 (Fig. 7), as described in Materials and Methods. As a control, potentiometric reductive titrations of membrane fragments with MBP protein alone were carried out, and only one redox species with an E_m of about +67 mV was calculated, which would be due to endogenous cytochrome of the bacterial cytoplasmic membrane (Fig. 7). When membrane fragments containing the chimeric MBP-Ssub*α*I17 were used, they exhibited two redox potentials species with E_m of +67 mV and +180 mV (Fig.7). The lower E_m component would correspond again to the endogenous cytochrome and the new component with the higher E_m to the

overexpressed and *in vivo* reconstitution of a chimeric homodimeric (*α/α*) Cyt b_{559} like structure. Note the good correlation between the ratio of the absorption changes of the chimeric and control membranes (Fig. 4, blue and black lines) and the changes corresponding to the +180 mV and +67 mV (Fig.7, black line) redox forms, in both cases the ratio was around 2.3-folds.

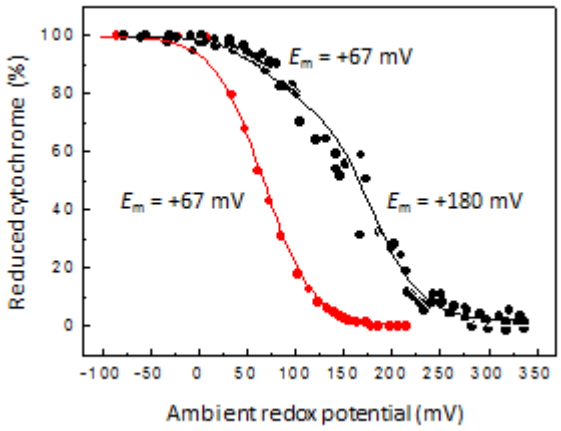

Fig.7*: Reductive potentiometric titrations of the cytochromes present in E. coli TB1 cytoplasmic membrane fragments. Redox titration was carried out in cytoplasmic membrane fragments containing either the MBP protein only (red) or the chimeric homodimer (αI17/αI17) Cyt* b_{559} *like structure (black), as described in Materials and Methods. The figure represents the plot of the percentages of reduced cytochromes obtained from the absorbance differences at 559–570 nm versus ambient redox potentials from the two redox titrations. Solid curves represent the best fits of the Nernst equation to the experimental data in accordance with one-electron processes (n = 1) for one (red line) or two (black line) components. For other details see Materials and Methods*

4. Discussion

In the present paper, we demonstrated that the full length *α*-subunit was unable to reconstitute a Cyt b_{559} like structure *in vivo* despite its incorporation and stabilization within the cytoplasmic membrane as shown by the SDS-PAGE analysis (Fig. 2b, lane 3). By contrast considering the high structural homology between both subunits, the situation with the full length *β*-subunit was completely different where the *in vivo* formation of a Cyt b_{559} like structure was indeed possible (Prodöhl et al. 2005; Luján et

al. 2012). According to the structure of the natural heterodimeric (*α/β*) Cyt b_{559} from cyanobacteria (Figs. 1 and 8), the position of two amphipathic short *α*-helices of the N-terminus full length *α*-subunit on the cytoplasmic membrane surface may block the entry of the heme to coordinate the two histidines to mature the chromoprotein (Fig. 8, *αα*). After rid of the complete out-of-membrane N-terminus part of the *α*-subunit, the *in vivo* reconstitution of a chimeric homodimeric (*α/α*) Cyt b_{559} like structure was well possible, as shown by the brownish color of the cell culture pellet, SDS-PAGE, immunoblots, partial purification, and absorption and EPR spectra. We think the elimination of the protein steric hindrance on the surface of the membrane at the entry of the heme, would now allow the free entrance of the heme group to coordinate to the two histidine ligands to mature a Cyt b_{559} like structure (Fig. 8, *α*I17*α*I17). This conclusion was highly reinforced by using

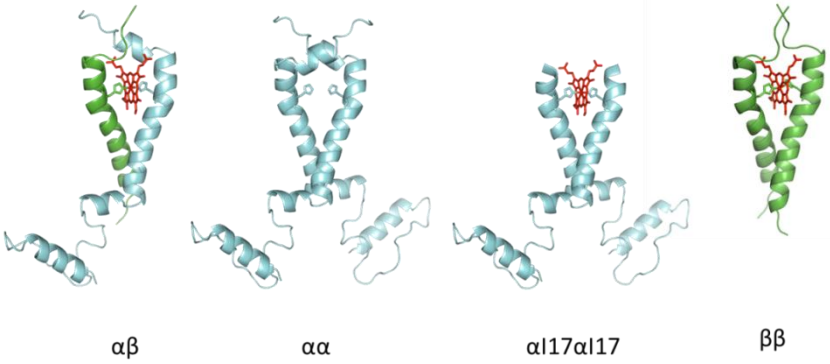

***Fig.8**: Ribbon representations of the different structures of Cyt b_{559}. αβ, natural Cyt b_{559} of the PSII core from T. vulcanus at 1.9 Å; αα, full length α-subunit homodimer; αI17αI17, chimeric α-subunit homodimeric Cyt b_{559} like structure; ββ, full length β-subunit homodimeric Cyt b_{559} like structure*

two additional N-terminus chimerics, one without the first eight amino acids but preserving the entire short amphipathic *α*-helix (called Ssub*α*P9), and the other without the first twelve amino acids preserving about half of the short *α*-helix (called Ssub*α*I13) (Fig. 9). In the case of the Ssub*α*P9, the reconstitution of a Cyt b_{559} like structure was not possible as in the case of the full-length *α*-subunit, but in the case of the Ssub*α*I13 a somewhat partial reconstitution was indeed possible. This strongly indicates that the presence of two entire amphipathic *α*-helices may block the entry of the heme group and interrupt the membrane-bound cytochrome maturation.

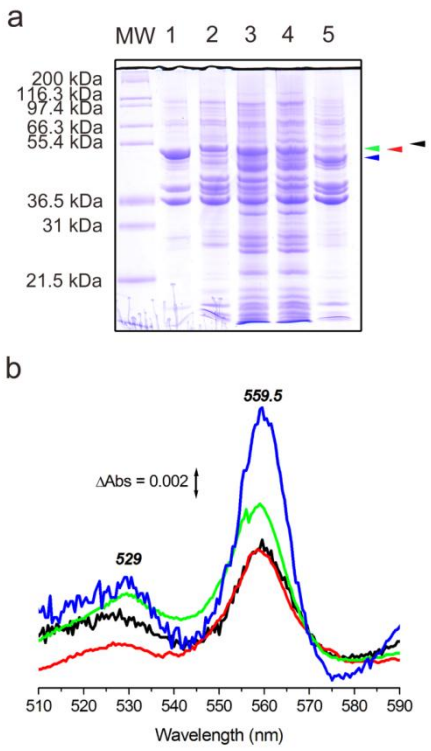

Fig.9: *Overexpression of different chimeric and full length α-subunits at 18 ºC. a, SDS-PAGE [12% (w/v) acrylamide, 4 M urea] analysis of bacterial membrane fragments: MW, molecular weight markers; lane 1, containing only the MBP (MBP-lacZ fusion protein of 50.8 kDa); lane 2, containing the MBP-full length Ssubα (fusion protein of 52.5 kDa; black color arrow); lane 3, containing the MBP- chimeric SsubαP9 (fusion protein of 51.7 kDa; green color arrow); lane 4, containing the MBP-chimeric SsubαI13 (fusion protein of 51.2 kDa; red color arrow); lane 5, containing the MBP-chimeric SsubαI17 (fusion protein of 50.7 kDa, bue color arrow). b, redox differential absorption spectra of the bacterial cytoplasmic membrane fragments within the 510-590 nm spectral range: containing MBP-full length Ssubα (black color line); the MBP-chimeric SsubαP9 (red color line); the MBP-chimeric SsubαI13 (green color line); the MBP-chimeric SsubαI17 (blue color line)*

Several attempts to overexpress the *α*-subunit without the MBP carrier were unsuccessful. In principle, one could think that the presence of a much bigger carrier protein compared to the *α*-subunit chimeric αI17 (42.5 *vs* 7.8 kDa) might interfere with a proper reconstitution of a Cyt b_{559} like structure. But this clearly seemed not to be the case in the present work. Indeed, the absorption spectra of the membranes overexpressing the chimeric fusion protein (Ssub*α*I17) identified a Cyt b_{559} like structure with the typical *α* and *β* spectral peaks at around 559 and 530 nm, respectively. The visible absorption spectra of the partially purified overexpressed chimeric fusion

protein along with the EPR characteristics and the redox potentiometric titration nicely confirmed the nature of the reconstituted form as a Cyt b_{559} like structure. Whether the MBP protein carrier might interfere with the heme assembly in the case of the full length native *α*-subunit but not with the *α*-chimeric is very unlikely since the MBP should be, in principle, closer to the heme niche in the chimeric compared to the full length α-subunit due to the lack of the N-terminus in the chimeric. Moreover, the use of this specific plasmid construct with the MBP carrier (Prodöhl et al. 2005; Kroliczewski et al. 2005; Dreher et al. 2007; Weber and Schneider 2013) assured that the reconstituted Cyt b_{559} like structures have a homogeneous orientation with the heme group towards the inner surface of the cytoplasmic bacterial membrane.

The E_m of about +30-50 mV, observed for the isolated natural Cyt b_{559} (Kaminskaya et al. 1999; Yruela et al. 2003) or the reconstituted form in solution (Luján et al. 2012), increased up to +180 mV in the *in vivo* reconstitution presented in this work, most probably due to the higher hydrophobicity imposed by the membrane lipid and the rearrangement of the heme pocket after its insertion within the membrane. However, in both the homodimeric (*β/β*) (Luján et al. 2012) and chimeric homodimeric (*α*I17/*α*I17) (present work) forms, the redox potentials were significantly lower than +300-400 mV, as observed for the HP form of the natural heterodimeric (*α/β*) Cyt b_{559} within the photosynthetic membrane (Stewart and Brudvig 1998; Roncel et al. 2003; Guerrero et al. 2014). The heme pocket generated in the *in vivo* homodimeric reconstitutions (Fig.8, *α*I17/*α*I17 and *β/β*) might be too open, increasing the exposition to the surrounding solvent and thus reducing its hydrophobicity and the redox potential of the heme (Krishtalik et al. 1993; Roncel et al. 2001). This situation might be overcome by the presence of an amphipathic *α*-helix that shields the heme niche from outside as in the case of the natural heterodimer (*α/β*).

Furthermore, our data suggest that the photosynthetic natural Cyt b_{559} assembly and maturation would most probably occur by a three step model as demonstrated for the (*β/β*) homodimer in (Volkmer et al. 2006; Ackdogan et al. 2012). First, the polypeptides enter the membrane matrix; second, an *α*-helix interacts with and recognizes another *α*-helix at the conserved glycine and phenylalanine residues near the thylakoid lumen surface to make a (*α/β*) heterodimer; and third, the heme group is incorporated to coordinate the two histidines and form a mature holoprotein. According to our data and other results (Volkmer et al. 2006); Ackdogan et al. 2012), the heme

group seems not to be necessary for the incorporation, recognition and stable assembly of the protein complex subunits. The consecutively maturation steps would be as the following:

$$\alpha\text{-subunit} + \beta\text{-subunit} \dashrightarrow (\alpha/\beta) + \text{heme} \dashrightarrow \text{Cyt } b_{559}$$

However, the proposed model cannot be generalized to other more complex cytochromes and chromoproteins and each protein has to be studied separately. For instance, in the case of the retinal, the sole chromophore of a more complex and well-known membrane-bound protein as bacteriorhodopsin with seven transmembrane α-helices, it was also no necessary for the formation of the protein folding structure within the membrane (Booth et al. 1995). But in the case of the photosynthetic light-harvesting complex (LHCII), the chomophores, chlorophylls and carotenoids, were indeed necessary for the polypeptide folding and protein complex maturation (Horn et al. 2007; Paulse et al. 1993).

Finally, in the present work we have tried to answer the question of why the full length α-subunit in contrast to the full length β-subunit, was unable to *in vivo* reconstitution of a Cyt b_{559} like structure, despite the high structural homology between these two subunits. Our hypothesis that a structural steric hindrance due to the presence of an out-of-membrane amphipathic α-helix was the cause of lack of the cytochrome maturation, is strongly supported by the results. The presence of that amphipathic α-helix might also affect the redox potential of the heme niche. The present structural work is even more relevant considering the scarce information available on integral membrane protein maturation as compared to the soluble ones. Weather this chimeric structure can be actually synthesized and assembled in a photosynthetic system and, more important, weather these homodimeric structures (chimeric αI17/αI17; β/β) could be functional photosynthetically remain to be proved. An on-going project in our laboratory is trying to respond to these interesting questions.

Acknowledgements

We thank P. Lorente for technical assistance. This work was supported by Grants from the Spanish Ministry of Economy and Competitiveness (MINECO) (AGL2011-23574, MAT2011-23861, BIO2012-35271, BFU2010-16297), the Aragón Regional

Government (E33 and B18), and the Andalucía Regional Government (PADI BIO-022). All these Grants were partially financed by the EU FEDER Program.

References

Ackdogan Y, Anbazhagan V, Hinderberger D, Schneider D (2012) Heme binding constricts the conformational dynamics of the cytochrome *b559´* heme binding cavity. Biochemistry 51: 7149-7156.

Ahmad I, Giorgi LB, Barber J, Porter G, Klug DR (1993) Redox potentials of cytochrome b-559 in the D1/D2/cytochrome b-559 reaction centre of photosystem II. Biochim Biophys Acta 1143: 239-242.

Alfonso M, Collados R, Yruela I, Picorel R (2004) Photoinhibition and recovery in a herbicide-resistant mutant from *Glycine max* (L.) Merr. cell cultures deficient in fatty acid unsaturation. Planta 219: 428-439.

Babcock GT, Widger WR, Cramer WA, Oertling WA, Metz JZ (1985) Axial ligands of chloroplast cytochrome *b*-559: identification and requirement for a heme-cross-linked polypeptide structure. Biochemistry 24: 3638-3645.

Booth PJ, Flitsch SL, Stern LJ, Greenhalgh DA, Kim PS, Khorana HG (1995) Intermidiates in the folding of the membrane protein bacteriorhodopsin. Nat Struct Biol 2: 139-143.

Dreher C, Prodohl A, Weber M, Schneider D (2007) Heme binding properties of heterologously expressed spinach cytochrome b_6: implications for transmembrane b-type cytochrome formation. FEBS Lett 581: 2647-2651.

Faller P, Pascal A, Rutherford AW (2001) β-carotene redox reactions in Photosystem II: electron transfer pathway. Biochemistry 40: 6431-6440.

Franke C, Loyal R, Ohad I, Haehnel W (1999) In vitro assembly of a β2 cytochrome-like complex from the chemically synthesized β-subunit encoded by the Synechocystis sp. 6803 *psbF* gene. FEBS Lett 442: 75-78.

García-Rubio I, Martínez JI, Picorel R, Yruela I, Alonso PJ (2003) HYSCORE spectroscopy in the cytochrome *b559* of the photosystem II reaction center. J Am Chem Soc 125: 15846-15854.

Guerrero F, Roncel M, Kirilovsky D, Ortega JM (2013) Site-directed mutagenesis of cytochrome *b*559 in the cyanobacterium *Thermosynechococcus elongatus.* In Kuang T, Lu C and Zhang L (eds.) Photosynthesis Research for Food, Fuel and Future. *Series: "Advanced Topics in Science and Technology in China"*. Berlin Heidelberg: Zhejiang University Press, Hangzhou and Springer-Verlag GmbH, pp. 71-74.

Guerrero F, Zurita JL, Roncel M, Kirilovsky D, Ortega JM (2014) The role of the high potential form of the cytochrome *b*559: Study of *Thermosynechococcus elongatus* mutants. Biochim Biophy Acta-Bioenergetics 1837: 908-919.

Guex N, Peitsch MC (1997) SWISS-MODEL and the Swiss-PdbViewer: An environment for comparative protein modeling. Electrophoresis 18: 2714-2723.

Guskov A, Kern J, Gabdulkhakov A, Broser B, Zouni A, Saenger W (2009) Cyanobacterial photosystem II at 2.9 Å resolution and the role of quinones, lipids, channels and chloride. Nat Struct Mol Biol 16: 334-342.

Horn R, Grundmann G, Paulsen H (2007) Consecutive binding of chlorophylls *a* and *b* during the assembly in vitro of light-harvesting chlorophyll-*a/b* protein (LHCIIb). J Mol Biol 366: 1045-1054.

Kaminskaya O, Kurreck J, Irrgang KD, Renger G, Shuvalov VA (1999) Redox and spectral properties of cytochrome b559 in different preparations of photosystem II. Biochemistry 38: 16223-16235.

Kamiya N, Shen JR (2003) Crystal structure of oxygen-evolving photosystem II from Thermosynechococcus vulcanusat 3.7 Å resolution. Proc Nat Acad Sci USA 100: 98-103.

Koua FHM, Umena Y, Kawakami K, Shen JR (2013) Structure of Sr-substituted photosystem II at 2.1 Å resolution and its implications in mechanism of water oxidation. Proc Nat Acd Sci USA 110: 3889-3894.

Krishtalik LI, Tae JS, Cherepanov DA, Cramer WA (1993) The redox properties of cytochromes b imposed by the membrane electrostatic environment. Biophys J 65: 184-195.

Kroliczewski J, Hombek-Urban K, Szczepaniak A (2005) Integration of the thylakoid membrane protein cytochrome b_6 in the cytoplasmic membrane of *Escherichia coli*. Biochemistry 44: 7570-7576.

Laskowski RA, MacArthur MV, Moss DS, Thornton JM (1993) PROCHECK - a program to check the stereochemical quality of protein structures. J App Cryst 26: 283-291.

Luján MA (2009) Overexpression, purification, and reconstitution of the cytochrome b559, Ph. D. thesis, The University of Zaragoza.

Luján MA, Martínez JI, Alonso PJ, Guerrero F, Roncel M, Ortega JM, Picorel R (2012) Reconstitution, spectroscopy, and redox properties of the photosynthetic recombinant cytochrome *b559* from higher plants. Photosynth Res 112: 193-204.

Nanba O, Satoh K (1987) Isolation of a photosystem II reaction center consisting of D1 and D2 polypeptides and cytochrome *b559*. Proc Nat Acad Sci USA 84: 109-112.

Paulsen H, Finkenzeller B, Kuhlein N (1993) Pigments induced folding of light-chlorophyll *a/b*-binding protein. Eur J Biochem 215: 809-816.

Picorel R, Chumanov G, Cotton TM, Montoya G, Seibert M (1994) Surface-enhanced resonance Raman scattering spectroscopy of photosystem II pigment-protein complexes. J Phy Chem 98: 6017-6022.

Prodöhl A, Volkmer T, Finger C, Schneider D (2005) Defining the structural basis for assembly of a transmembrane cytochrome. J Mol Biol 350: 744-756.

Roncel M, Ortega JM, Losada M (2001) Factors determining the special redox properties of photosynthetic cytochrome *b*559. Eur J Biochem 268: 4961-4968.

Roncel M, Boussac A, Zurita JL, Bottin H, Sigiura M, Kirilovsky D, Ortega JM (2003) Redox properties of the photosystem II cytochromes b559 and c550 in the cyanobacterium *Thermosynechococcus elongates.* Biol Inorg Chem 8: 206-216.

Sagasti S, Yruela I, Bernal M, Lujan MA, Frago S, Medina M, Picorel R (2011) The Copper Chaperone for the Coppe/Zinc Superoxide Dismutase (CCS) from *Glycine max.* Metallomics 3: 169-175.

Seibert M, Picorel R (2011) Isolation of photosystem II reaction center complexes from plants. In Carpentier R (ed.) Methods in Molecular Biology 684. Photosynthesis Research Protocols 2nd edition, Humana Press, NY, pp.17-27.

Shinopoulos KE, Brudvig GW (2012) Cytochrome *b559* and cyclic electron transfer within photosystem II. Biochim Biophys Acta 1817: 66-75.

Shuvalov V, Fiege R, Schreiber U, Lendzian F, Lubitz W (1995) EPR study on cytochrome in the D1D2 Cyt *b-559* complex. Biochim Biophys Acta 1228: 5-180.

Stewart DH, Brudvig GW (1998) Cytochrome *b559* of photosystem II. Biochim Biophys Acta 1367: 63-87.

Sugiura M, Nakamura M, Koyama K, Boussac A (2015) Assembly of oxygen-evolving Photosystem II effeciently occurs with the apo-Cyt b_{559} but the holo-Cyt b_{559} accelarates the recovery of a functional enzyme upon photoinhibition. Biochim Biophys Acta 1847: 276-285.

Umea Y, Kawakami JR, Shen JR, Kamiya N (2011) Crystal structure of oxygen-evolving photosystem II at a resolution of 1,9 Å. Nature 473: 55-61

Van Gunsteren WF, Billeter SR, Eising AA, Hunenberguer, PH, Kuger P, Mark AE, Scott WRP, Tironi IG (1996) Biomolecular simulation: The GROMOS96

Manual and User Guide, Vdf Hochschulverlag AG der ETH Zurich, Zurich, Switzerland, pp. 1-1042.

Volkmer T, Becker C, Prodöhl A, Finger C, Schneider D (2006) Assembly of a transmembrane b-type cytochrome is mainly driven by transmembrane helix interactions. Biochim Biophys Acta 1758: 1815-1822.

Weber M, Schneider D (2013) Six amino acids define a minimal dimerization sequence and stabilize a transmembrane helix dimer by close packing and hydrogen bonding. FEBS Lett 587: 1592-1596.

Yruela I, Gracía-Rubio I, Roncel M, Martínez JI, Ramiro MV, Ortega JM, Alonso PJ, Picorel R (2003) Detergent effects on cytochrome b559 electron paramagnetic resonance signals in the photosystem II reaction center. Photochem Photobiol Sci 2: 437-442.